scientific reports

Check for updates

OPEN

Optimizing interval type-2 fuzzy logic PID controller with an improved constraint differential evolution algorithm

Xin Chen[1], Haozhen Dong[2], Chen Shen[3], Hanyu Li[2] & Dong Li[4]✉

Compared to electric actuators, hydraulic actuators can deliver greater driving forces within limited spaces due to their high-power density characteristics, making them widely used in high-performance drive applications such as humanoid robots. However, these systems exhibit significant nonlinear dynamic properties, posing challenges for high-precision control of their output forces. To address the control challenges of hydraulic actuators for humanoid robots, this paper first establishes a system model integrating the hydraulic power source with nonlinear hydraulic cylinders. Subsequently, an improved constrained differential evolution with better and nearest option (ICBNDE) algorithm is proposed, featuring an efficient search mechanism and an approximate solution selection strategy. Then, an interval type-2 fuzzy logic PID controller (IT2FL-PID-C) optimized by ICBNDE is constructed for the closed-loop control of the hydraulic actuator system. To validate the proposed algorithm's performance, the convergence and feasibility analyses of ICBNDE are conducted on the CEC2006 constrained benchmark test. Subsequently, the designed controller is compared with a traditional PID controller, and ICBNDE is contrasted with several classical constrained optimization algorithms under identical architectures. Furthermore, a comparative analysis of different membership functions for the IT2FL-PID-C is presented. Experimental results demonstrate that the ICBNDE based IT2FL-PID-C significantly outperforms traditional PID methods in both control accuracy and system stability. Moreover, ICBNDE exhibits superior robustness and repeatability in controller parameter optimization, achieving better median and mean performance with lower variance compared to other algorithms, which validates its effectiveness and reliability for controlling complex nonlinear hydraulic systems.

Keywords Interval type-2 fuzzy logic PID controller, Constraint differential evolution, Better and nearest option, Hydraulic actuator

With the continuous advancement of robotics technology, hydraulic actuators have emerged as a vital power solution for high-performance robotic drive systems. Their high-power density enables significantly greater output power than electric actuators within confined spaces. A series of hydraulic robotic platforms, such as Boston Dynamics' ATLAS[1] and Big Dog[2], as well as the HyQ developed by the Italian Institute of Technology[3], have fully demonstrated the technical feasibility of hydraulic drives under dynamic motion and complex load conditions. However, the design and control of hydraulic systems still face critical challenges. First, the hydraulic power source, as a core component of the system, must move in coordination with the robotic platform, presenting significant difficulties in achieving compactness, lightweight design, and energy efficiency optimization. Second, hydraulic actuators—particularly hydraulic cylinders—exhibit strong nonlinear dynamic characteristics, making it difficult for traditional linear control strategies like PID to achieve ideal control performance[4]. Fuzzy logic controllers (FLCs), as an effective method for handling nonlinear and uncertain problems, have been successfully applied in various engineering fields, including classification systems, wireless sensor networks[5], adaptive fuzzy control with predefined-time convergence[6], power system regulation[7], robot control[8], and hydraulic systems[9]. Compared to Type 1 Fuzzy Logic Controllers (T1FLC), Interval Type 2 Fuzzy Logic Controllers (IT2FLC) offer superior robustness and adaptability in handling information uncertainty and

[1]School of Mechanical and Electronic Engineering, Wuhan Business University, Wuhan 430056, China. [2]CASIC Research Institute of Intelligent Decision Engineering, Wuhan 430040, China. [3]School of Intelligent Manufacturing, Wuhan Railway Vocational College of Technology, Wuhan 430205, China. [4]School of Mechanical and Electronic Engineering, Wuhan City Polytechnic, Wuhan 430070, China. ✉email: 99956835@qq.com

modeling system nonlinearity[10]. These characteristics endow IT2FLC with significant potential for hydraulic system control. Therefore, this paper focuses on researching IT2FLC control methods for hydraulic cylinder actuators, aiming to enhance the control accuracy and dynamic performance of hydraulic drive systems in robotic applications. This research holds significant theoretical value and engineering significance for advancing hydraulic robotics technology.

Although the Interval Type-2 Fuzzy Logic Controller (IT2FLC) demonstrates significant advantages in hydraulic control, its numerous parameters make tuning considerably more challenging than for traditional PID controllers. Currently, optimization methods for IT2FLC can be broadly categorized into three types: mathematical optimization, meta-heuristic optimization algorithms, and hybrid methods. Most mathematical optimization methods rely on gradient information, yet they perform poorly when addressing the high-dimensional optimization problems associated with IT2FLC[11]. Although approximate gradients are widely used in mathematical optimization, they are prone to getting stuck in local optima during the solution process, thereby limiting the accuracy of the obtained solutions. In contrast, most metaheuristic methods do not rely on gradient information of the objective function. Through multiple iterations, they can effectively obtain approximate optimal solutions, demonstrating good applicability in IT2FLC optimization. With advances in computational technology, the time cost of metaheuristic algorithms has been significantly reduced, making them the most widely applied category of methods in current IT2FLC design[12]. Among these, methods such as Genetic Algorithms (GA), Particle Swarm Optimization (PSO), Chemical Reaction Optimization (CRO), and Bacterial Foraging Optimization Algorithm (BFOA) have been practically applied in IT2FLC design. To systematically review the research progress on this optimization problem, this paper provides a brief overview of the aforementioned meta-heuristic-based IT2FLC optimization methods.

a) Genetic Algorithm (GA).

GA is among the earliest algorithms explored for optimizing average-type type-2 fuzzy logic controllers (AT2FLCs). Maldonado[13] proposed using a multi-objective GA to optimize an AT2FLC for DC motor speed control, where the objective function is the weighted sum of multiple performance metrics, as shown in Eq. (1):

$$\mathrm{U} = \sum {}_{i=1}\omega_i f_i \tag{1}$$

Where, ω_i denotes the fixed weight coefficient, while f_i represents various performance metrics such as overshoot, undershoot, and steady-state error. To validate the superiority of the designed GA-optimized AT2FLC, the optimized AT2FLC with a Type-1 Fuzzy Logic Controller (T1FLC) was compared with a conventional PID controller. The experimental results demonstrated that the AT2FLC outperformed both in terms of control performance. Addressing control requirements in baking applications, Li et al.[14] proposed a T2FLC method based on Single Input Rule Modules (SIRM) for trailer system control. This approach utilizes GAs to optimize the membership function parameters, scaling factors, and SIRM parameters within the T2FLC. The system defines three primary control objectives: vertical position, trailer angle, and relative angle. The fitness function is expressed as Eq. (2):

$$\mathrm{J} = \sum {}_{s=1}^{S}(\gamma_\alpha IAE_s(\alpha) + \gamma_\beta IAE_s(\beta) + \gamma_y IAE_s(y)) \tag{2}$$

Where S denotes the number of different initial conditions, γ is the weight factor. And α, β, y represent three control objectives mentioned above respectively. Li compared the proposed SIRM-connected T2FLC with T1FLC, and the simulation results revealed that SIRM-connected T2FLC outperform T1FLC in the time cost of the truck-trailer system.

b) Particle Swarm Optimization (PSO).

Hamza et al.[15] proposed a PSO algorithm to optimize the parameters of the interval type-2 fuzzy proportional-derivative controller (IT2F-PD-C) in a rotating inverted pendulum (RIP) system. The fitness function employed in this study is shown in Eq. (3):

$$\mathrm{cost} = \frac{1}{2}(Mp + Ess + Eu) - \frac{e^{-\gamma}}{2}(Tr - Ts + Ess + Mp) \tag{3}$$

Where, Ess denotes steady-state error, Ts represents settling time, Tr denotes rise time, Mp indicates maximum overshoot, Eu signifies control energy consumption, and γ represents the corresponding weight coefficient. To validate the performance of the PSO algorithm, the authors compared it with the GA. Simulation results indicated that while both algorithms effectively optimize the IT2F-PD-C controller, PSO demonstrates superior performance across three metrics: overshoot, settling time, and control energy consumption. GA only slightly outperforms PSO in terms of steady-state error.

Allawi[16] applied PSO to optimize the IT2FLC and validated it through multiple experiments in multi-mobile robot systems. This research focused on robot cooperative control and target-reaching tasks, employing a fitness function defined as the sum of squared collision times, as shown in Eq. (4):

$$\mathrm{fitness}_i = \frac{1}{2}\sum {}_{j=1,j\neq i}^{n}\left(\frac{k}{Tc_{ij}}\right)^2 \tag{4}$$

where n denotes the number of robots, Tc_{ij} represents the predicted collision time between the i-th and j-th robots, and k is a finite constant. Experiments were conducted using two E-puck mobile robots. Results

demonstrate that the PSO-optimized IT2FLC effectively enhances navigation efficiency and collaborative performance.

c) Other algorithms.

Kiani et al.[17] proposed using the bacterial foraging optimization algorithm (BFOA) to optimize the IT2FLC and applied it to an automatic voltage regulation system. In this study, BFOA was employed to tune the membership function parameters of the IT2FLC. To better adapt the BFOA algorithm to this control problem, researchers designed an adaptability function of the following form, as shown in Eq. (5):

$$\mathrm{J}\,(\mathrm{k}) = G_e \int_0^T e^2\,(t)\,dt + G_u \int_0^T u^2\,(t)\,dt + G_M M_p \tag{5}$$

Where $e\,(t)$ denotes the system error, $u\,(t)$ represents the output signal of the IT2FLC, T is the system runtime, and M_p is the overshoot percentage; G_e, G_u, and G_M denote the corresponding weighting coefficients. Simulation results demonstrated that the BFOA-optimized IT2FLC performs well in automatic voltage regulation systems, particularly in noisy environments, exhibiting superior control performance compared to the Extended Discrete Action Reinforcement Learning Automata (EDARLA) method.

d) Hybrid algorithm.

Fayek et al.[18] proposed a hybrid optimization strategy combining PSO and GA, applying it to parameter tuning of the IT2FLC in DC servo motor position control. In this study, the decision variables were set as the input/output gains of the IT2FLC and its membership function (MF) parameters. The objective function was formulated as a multi-objective weighted form, corresponding to two experimental phases as shown in Eqs. (6) and (7):

$$FE = O_1 - 0.5O_2 \tag{6}$$

$$O_i = IAE = \sum\nolimits_{k=1}^{n} |e\,(k)| \tag{7}$$

Where O_1 and O_2 represent the objective function values for the first and second experimental phases, respectively; $e\,(k)$ denotes the error between the target value and the actual output at the k-th sampling point; and n is the total number of sampling points.

Furthermore, Arega et al.[19] proposed a novel approach combining a neural network-based nonlinear PID controller with backstepping control techniques in their experimental study on trajectory tracking for wheeled robots. The neural network-based nonlinear PID controller was trained and developed using input and output data. Subsequently, the neural network was trained using a Bayesian regularization algorithm. This study addressed the limitations of traditional PID controllers in complex, nonlinear systems by employing various advanced intelligent control strategies to achieve superior performance.

Based on the above analysis, the optimization of IT2FLC typically falls under multi-objective optimization problems. In practical control system design, two fundamental requirements must be balanced: tracking performance and stability performance. The former aims to ensure the system output accurately tracks the target signal with minimal error, while the latter requires the system to rapidly stabilize upon receiving a termination command and exhibit low steady-state error. Currently, most studies employ the weighted factor method to transform multi-objective problems into single-objective ones for solution. This approach is widely adopted for two primary reasons: First, single-objective meta-heuristic algorithms based on weighted factors are generally simpler to implement than multi-objective algorithms[20]. Second, in most hydraulic control problems, the practical engineering requirement is to obtain an IT2FLC solution with excellent overall performance, whereas the Pareto solution set generated by multi-objective optimization is not applicable in such scenarios[21]. However, the weighted factor method also introduces a critical issue: how to reasonably design the weighted fitness function and determine its factor values. Currently, such parameters are largely set based on expert experience, lacking systematic determination criteria, which can easily lead to controversial results. Additionally, converting multi-objective problems into constrained single-objective problems represents another common engineering approach independent of weighting factors, though its application in IT2FLC optimization remains limited. Given this context, this paper employs an improved constrained heuristic algorithm to optimize IT2FLC, aiming to provide valuable references for its theoretical expansion and engineering applications in hydraulic control.

In summary, this paper proposes an improved constrained differential evolution with better and nearest option (ICBNDE) algorithm with enhanced solution approximation capabilities. It is applied to optimize an Interval Type-2 Fuzzy Logic PID Controller (IT2FL-PID-C) for achieving high-precision control of hydraulic cylinder positioning. The paper is structured as follows: Sect. "Hydraulic system in humanoid robot" introduces the self-designed mobile hydraulic power unit and related hydraulic system models; Sect. "Constraint differential evolution with better and nearest option of NBDE" elaborates on the fundamental principles and implementation framework of the ICBNDE algorithm; Sect. "IT2FL-PID-C based hydraulic system optimization" proposes a hydraulic control strategy based on IT2FL-PID-C and its optimization method; Sect. "Experiments and analysis" presents simulation results, including statistical performance analysis of ICBNDE in benchmark tests and comparative evaluations between ICBNDE-IT2FL-PID-C and other IT2FL-PID-C-based algorithms; the final section concludes with a summary and future research directions.

Hydraulic system in humanoid robot

The hydraulic system principle of the humanoid robot designed in this paper is shown in Fig. 1. Similar to most hydraulic robots, this system primarily consists of two major components: the hydraulic power unit and the servo

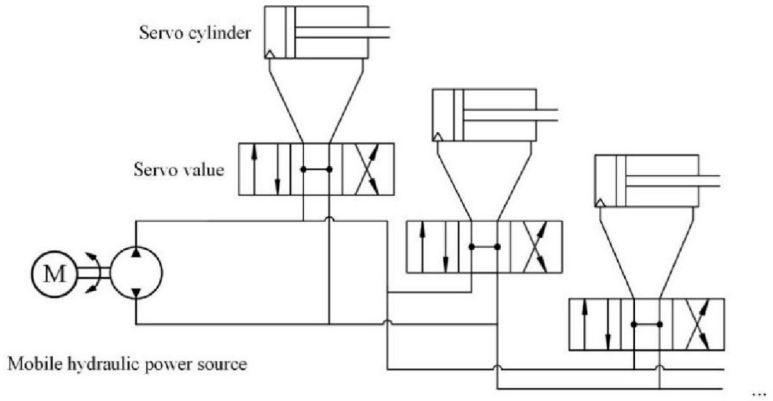

Fig. 1. Hydraulic schematic of humanoid robot.

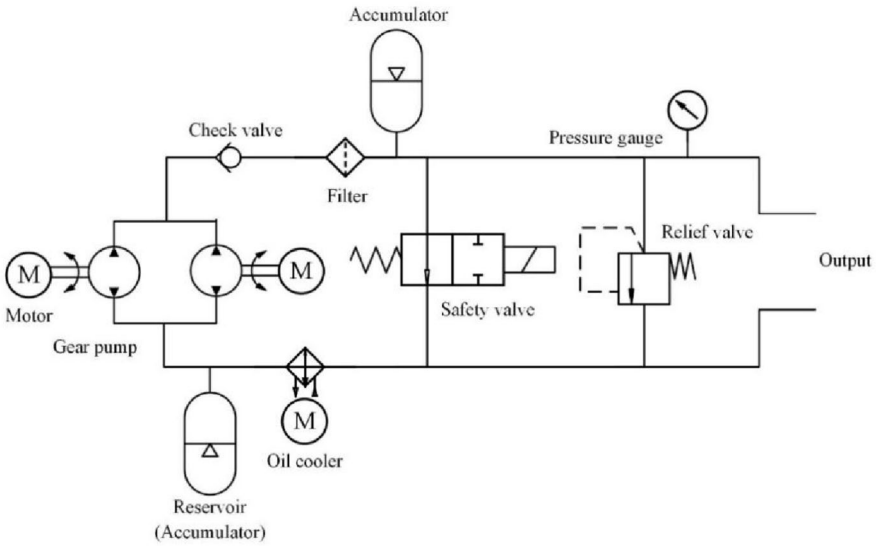

Fig. 2. Working principle diagram of mobile hydraulic power source.

hydraulic unit. This section will sequentially elaborate on these two components and establish a mathematical model for the servo hydraulic cylinder based on this foundation.

Mobile hydraulic power source

In mobile equipment, the hydraulic power source needs to be designed to be compact and easy to carry. For a humanoid robot, many design issues such as the size and mass, output flow and pressure, and cooling power should be considered in mobile power source design. The size and mass of the power source are limited. Otherwise, it may hardly be installed in a human robot. Sufficient output power can guarantee the locomotion ability and stability of a humanoid robot. Besides, ample cooling power will prolong stability period of robot hydraulic system.

Figure 2 shows the working principle of a hydraulic power source, which is constructed with two motors, two gear pumps, a filter, two accumulators, a pressure gauge, a check value, a safety value, a relief value, and an oil cooler. The relevant performance parameters of these elements are shown in Table 1. In the mobile hydraulic power source, two brushless motors are used as the power source, because each motor can provide 4.4 kW power within a limited size. Two Marzocchi gear pumps work to transferring the mechanical energy to hydraulic energy. Because the maximum input rpm of this kind of gear pump matches the maximum output rpm of the electrical motor, the decelerator does not need to be connected. Two accumulators as the reservoirs will ensure the oil supply capacity. To improve the cooling efficiency, an oil cooler with high heat dissipation power and the hydraulic oil with high working temperature are used. After these designs, the size of this mobile hydraulic power source is limited to 520 × 405 × 110 mm, and its mass is limited to 15.8 kg. The continuous maximum output power is expected to be 18 L/min with 18 Mpa and is sufficient for the power output of our humanoid robot[22].

Name	Manufacturer	Model	Main parameters
Motor	Scorpion	SII-6530-180KV	12s, 4.8KW, 180KV
Pump	Marzocchi	K1P-R2.5XG	1.6 cc, 6000Rpm
Check Valve	Mirco-hydraulic	MVC-5	0.2 bar
Relief Valve	Sun-hydraulic	RDBALWN	12gpm
Safety Valve	Sun-hydraulic	DTAFMCN-224 L	7gpm
Accumulator	HADAC	SBO210-0.32E1/112A9-210AK	0.32 L, 210 bar
Reservoir	Mirco-hydraulic	MT-0.63	0.63 L, 0.4 bar
Filter	HAWE	PFM4-F510-R4D	10μ m

Table 1. Hydraulic components and its parameters.

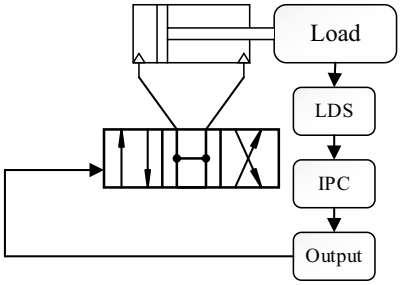

Fig. 3. Electronic control system of hydraulic cylinder.

Nonlinear hydraulic cylinder system

In the above work, the power source can provide sufficient power for our humanoid robot. The dynamic property of cylinder is sensitive to its input hydraulic power[23]. Without a powerful hydraulic power source, the working state of the whole hydraulic system may decrease, and IT2FL-PID-C optimization may be meaningless. In order to demonstrate that IDSO based IT2FL-PID-C design method will perform well in the humanoid robot hydraulic system, the hydraulic cylinder is firstly modeled, which will be used for the IT2FL-PID-C optimization test.

As shown in Fig. 3, this electronic control system constitutes a typical closed-loop control system, primarily comprising a linear displacement sensor (LDS), an industrial personal computer (IPC), an output module (Output), a hydraulic cylinder, a servo valve, and a load. This system has been extensively applied in controlling multiple joints of the humanoid robot under study, specifically including the pitch and roll degrees of freedom of the ankle joint, as well as the pitch and yaw degrees of freedom of the knee joint.

The hydraulic system transfer function employed in the IT2FL-PID-C optimization is shown in Eq. (8), which is a general theoretical model used to describe the dynamic characteristics of hydraulic systems. The specific parameter values in Eq. (9) are derived from the technical data sheets provided by the experimental system and the reference hydraulic component manufacturer. Here, Y denotes the actual displacement of the hydraulic cylinder, ω ? represents the system's natural frequency, ϵ ? is the damping coefficient. The specific values of these parameters are estimated by applying step signals or swept-frequency signals to the hydraulic cylinder in the experimental system, measuring its displacement response, and then utilizing methods such as the least squares method. F indicates the load force (which can be considered zero under the experimental conditions) and K_Q is the flow gain of the servo valve, which are related to the specific model of the hydraulic cylinder. A_1 and A_2 represent the effective areas of the inner and outer diameters of the hydraulic cylinder, respectively. Their specific values are determined by the cylinder model. This characteristic constitutes one of the primary sources of nonlinearity in hydraulic systems[24]. In previous studies, to facilitate PID controller design, A was often assumed to be a large value to ensure system stability[25]. Since PID is a linear controller, simplified transfer functions typically suffice for parameter tuning[26]. However, the IT2FL-PID-C controller investigated herein is a nonlinear controller aimed at further enhancing control performance. Therefore, a more precise hydraulic cylinder model reflecting its actual dynamic characteristics is required.

$$\mathrm{Y} = \frac{\frac{K_Q I}{A_1} - \frac{F}{{A_2}^2}\left[K_{ce} + \frac{V_t}{2\left(1+n^2\right)\beta_e}s\right]}{s\left(\frac{s^2}{\omega_h^2} + \frac{2\epsilon_h}{\omega_h}s + 1\right)} \tag{8}$$

$$\omega_h = 252.9, \epsilon_h = 0.15, A_1 = 1.13 \times 10^{-4}, A_2 = 6.28 \times 10^{-5}, K_Q = 1.087 \times 10^{-2} \tag{9}$$

Constraint differential evolution with better and nearest option of NBDE

Unlike traditional differential evolution (DE) algorithms, the Nearest-Neighbor Differential Evolution (NBDE) employs a specialized mutation strategy termed "DE/rand-to-nearest-and-better/2." This strategy integrates concepts from both classical DE algorithms and the Whale Swimming Algorithm (WSA)[27,28]. Experiments on benchmark functions demonstrate that NBDE exhibits stable optimization performance and excellent convergence when handling multimodal problems. Compared to several other algorithms, NBDE is not only simpler to implement but also demonstrates superior convergence properties. The following sections first briefly introduce the three key components of NBDE—mutation, crossover, and selection—before elaborating on the overall architecture of the improved ICBNDE algorithm.

Mutation strategy

In the Differential Evolution (DE) algorithm, the mutation strategy serves as the core mechanism for generating candidate individuals and is a critical component enabling meta-heuristic algorithms to achieve a balance between global search and local exploitation. Among these, "DE/rand/1" stands as the most widely applied mutation strategy within classical DE and its numerous derivative algorithms. Its mathematical expression is shown in Eq. (10):

$$v_i^{G+1} = x_{r1}^G + F \times \left(x_{r2}^G - x_{r3}^G\right) \tag{10}$$

Where, G denotes the number of iterations, $r1$, $r2$, $r3$ represent the random IDs of individuals selected for the mutation process. F is the mutation operator parameter and it can be set to 0.5 in classical DE.

Inspired by conventional DE and WSA, a novel mutation strategy for individual generation is proposed, which can be shown in Eq. (11):

$$v_i^{G+1} = x_{r1}^G + rand\,(0,1) \times \left(x_{r2}^G - x_i^G\right) + rand\,(0,1) \times \left(y_i^G - x_i^G\right) \tag{11}$$

Consistent with the fundamental framework of the DE algorithm, G denotes the current evolutionary generation, while $r1$ and $r2$ represent the indices of randomly selected individuals within the population. Notably, y_i^G is defined as a reference individual that possesses "superior fitness and a spatially closer position" relative to the target individual x_i^G. When x_i^G itself is the current optimal individual, a randomly selected individual is used as a replacement to maintain population diversity and prevent premature convergence.

Crossover

The crossover operator plays a pivotal role in balancing convergence and diversity within differential evolution algorithms. This study employs a hybrid crossover strategy integrating three distinct crossover mechanisms. The specific process is as follows: First, a random number is generated to determine which crossover operator to apply between the candidate vector and the original target vector. Subsequently, based on the value of this random number, the system selects among binary crossover, exponential crossover, and the "non-crossover" operation. Finally, after completing the selected crossover operation, a new generation of candidate individuals v_i^{G+1} is generated.

The binary crossover operator is shown as Eq. (12):

$$v_{i,j}^{G+1} = \begin{cases} v_{i,j}^{G+1}, & if\ rand \leq\ CR \\ v_{i,j}^{G}, & otherwise \end{cases} ,\forall\, i \in\ NP; \forall\, j \in\ D \tag{12}$$

Where rand denotes a uniformly generated random number within the interval [0, 1], NP represents the size of the evolutionary population, and D is the dimension of the problem to be optimized. In Eq. (13), C_r serves as the crossover probability parameter in the CNBDE algorithm. Its value is typically set as a random number between 0.1 and 0.6, a range validated as suitable for most optimization problems.

$$Cr_j = \begin{cases} 1, & if\ rand \leq\ CR \\ 0, & otherwise \end{cases} ,j \in\ D \tag{13}$$

The pseudo exponential crossover operator we used as Table 2.

Selection

After generating candidate individuals v_i^G, the algorithm will evaluate their fitness. Subsequently, based on the tournament selection mechanism, two individuals are randomly selected from the population, with the one exhibiting superior fitness being retained for the next generation.

Framework of ICBNDE

Most optimization problems are constrained optimization problems (COPs). The strategy of using evolutionary algorithm to solve COPs can be roughly divided into two categories: penalty function strategy and multi-objective optimization technique[29]. Penalty function methods use the strategy that the constraint violations will add to the fitness value. The weight factor method keeps these individuals with significant constraint violation from surviving into the next generation. These methods have attracted researchers' attention and are applied to many different heuristic algorithms for COPs, such as[30,31]. For IT2FLC optimization problems, most researchers have also chosen this kind of method for the reason that penalty function is easy to implement. Although penalty

Algorithm 1

1. Generate a randomly vector C_r by Eq.13;
2. $M = Sum(C_r)$;
3. Generate a randomly number rand in [1, D];
4. for $j = 1$ to D
5. if j is not between $[rand, rand + M - 1]$
6. $v_{i,j}^{G+1} = x_{i,j}^{G}$
7. end if
8. end for

Remark: if rand+$M - 1 > D$, the judgment in line 5 can be rewritten in the following form: If $j < rand$ *and* $j > rand + M - D - 1$.

Table 2. The pseudocode of Algorithm 1.

function methods are efficient for most problems, the main limitation is that the weight factors require fine tuning. Multi-objective optimization method is another efficient method for COPs. The main idea is to transfer COPs into unconstrained multi-objective optimization problems. Although the multi-objective methods were questioned in the early years[32,33], they have been accepted by most researchers in recent years, because recent researches prove that this method is of high efficiency. The main advantage is that it is not a parameter-based method. The tuning of this method is easier than penalty function methods.

The CW approach is a classical approach proposed by Cai and Wang[34]. In the CW approach, the degree of constraint violation is shown as Eq. (14):

$$\mathrm{G}(\mathrm{x}) = \begin{cases} \max(0, g_i(x)) \\ max(0, |h_i(x)| - \delta) \end{cases} \tag{14}$$

Where $g_i(x)$ denotes the *i-th* inequality constraint and $h_i(x)$ is the *i-th* equality constraint. δ is the positive tolerance for equality constraint. Based on the CW approach and NBDE, we propose a novel algorithm named improved constraint differential evolution with better and nearest option (ICNBDE) for COPs. The core novelty of ICBNDE lies in its unique integration of a group-based search architecture with a multi-objective inspired constrained handling technique and a specific greedy local enhancement strategy. This synergistic combination is designed to effectively balance exploration and exploitation specifically for the high-dimensional, constrained, and potentially multi-modal parameter space of IT2FL-PID-C optimization. Several improvements are shown as follows:

a. To improve the searching ability of ICBNDE, the population size is enlarged. The individuals of ICBNDE are divided into several groups. The mutation operation, crossover operation, and selection operation will be implemented in their respective groups. This group-based niching strategy helps maintain population diversity and facilitates parallel exploration of different regions of the search space, which is crucial for avoiding premature convergence in complex problems. Then, the individuals will be regrouped after certain iterations.
b. Searching better and nearest individual for each individual is hard. So the mutation strategy is different from NBDE, and it can be written as Eq. (15):

$$v_{k.i}^{G+1} = x_{r1}^{G} + rand(0,1) \times \left(x_{R1}^{G} - x_{k,i}^{G}\right) + rand(0,1) \times \left(y_{k,i}^{G} - x_{k,i}^{G}\right) \tag{15}$$

Where x_{R1}^{G} is the random individual selected from the *k-th* group, and x_{r1}^{G} denotes the individual selected from the whole group. $y_{k,i}^{G}$ is a random individual selected from the individuals in *k-th* group with better fitness value compared with $x_{k,i}^{G}$. This hybrid mutation leverages both intra-group information x_{R1}^{G}, $y_{k,i}^{G}$ for focused exploitation and inter-group information x_{R1}^{G} for exploration.

c. Different from NBDE, the selection strategy can be summarized as follows: when both $x_{k,i}^{G}$ and $v_{k,i}^{G+1}$ are feasible, the individual with better fitness value will survive; when $x_{k,i}^{G}$ is infeasible and $v_{k,i}^{G+1}$ is feasible, $v_{k,i}^{G+1}$ will survive. When both of them are infeasible, the individual with the smaller sum of constraint violation will survive. This feasibility-prioritizing rule directly embeds the principles of constrained optimization without requiring penalty factor tuning.
d. To converge faster, a new greedy selection strategy similar to CMODE is proposed. When no selection operation happening in a group's evolution generation, which indicates a potential stagnation in that subgroup, a random number is generated to determine whether the following strategy will be implemented: Collect the non-dominated individuals $D_1, D_2, \ldots, D_N$ from the candidate individuals; Randomly replace the indi-

viduals in original group which are dominated by $D_1, D_2, \ldots, D_N$. This mechanism injects high-quality genetic material into stagnating groups, promoting local refinement. The trigger condition occurs when no candidate offspring in a group outperforms its parent in the current generation. In our experiments on the IT2FL-PID-C problem, this condition was triggered in approximately 15–25% of group generations, providing a balanced frequency of intervention that aids convergence without excessively disrupting population diversity. The probability p controls the activation rate of this greedy strategy. The greedy strategy probability p was set to 0.3 for problems with equality constraints and 0.2 otherwise, based on the observation that equality constraints often require more aggressive feasibility search. The algorithm's performance shows moderate robustness to p within ±0.1 of these values. The parameter settings for ICBNDE, including the group count (Gro = 8) and size (GroNP = 15), were determined through preliminary empirical tests on a subset of CEC2006 benchmarks. While performance is not critically sensitive to minor variations, significantly reducing the number of groups may diminish the niching effect, and overly large groups may slow down convergence.

The pseudo code of ICBNDE is shown as Table 3. Where Gro represents the number of groups, $GroNP$ represents the number of individuals in each group.

IT2FL-PID-C based hydraulic system optimization

As shown in Eq. (16), the IT2FL-PID-C based hydraulic system uses the target displacement Y_d^{cy} of the hydraulic cylinder as input and the actual displacement Y_a^{cy} as output. The controller's inputs include the error E between target and actual displacement, along with the differential of the error dE. Its outputs are U_{PI} and U_{PD}, respectively. The final control action U of the IT2FL-PID-C is formed by the integral summation of U_{PD} and U_{PI}.

$$U = U_{PD} + \sum U_{PI} \tag{16}$$

The PI and PD parts share the same MFs, and fuzzy rules are this IT2FL-PID-C. The closed-loop control system for the hydraulic cylinder based on IT2FL-PID-C is shown in Fig. 4.

Algorithm 2

Input: The objective function, the parameters of the ICBNDE.

Output: The global optimal solution.

1. Initialize the parameters of ICBNDE;
2. Create a set of initial solutions;
3. Calculate the fitness value and constraint value of the individual;
4. When the iteration stops
5. while $k = 1 \leq Gro$
6. for $i = 1$ to $GroNP$
7. Create a new individual $v_{k,i}^{G+1}$ according to Eq.15;
8. Implement crossover operation between $v_{k,i}^{G+1}$ and $x_{k,i}^{G}$;
9. Bound correction for $v_{k,i}^{G+1}$;
10. Evaluate $v_{k,i}^{G+1}$'s fitness value and constraint value;
11. if $v_{k,i}^{G+1}$ outperform than $x_{k,i}^{G}$
12. $x_{k,i}^{G+1} = v_{k,i}^{G+1}$
13. else
14. $x_{k,i}^{G+1} = x_{k,i}^{G}$
15. end if
16. end for
17. end while
18. if there is no replacement happens in k-th group and $rand < p$
19. Execute the greedy selection strategy
20. end if
21. end while

Table 3. The pseudo of ICBNDE.

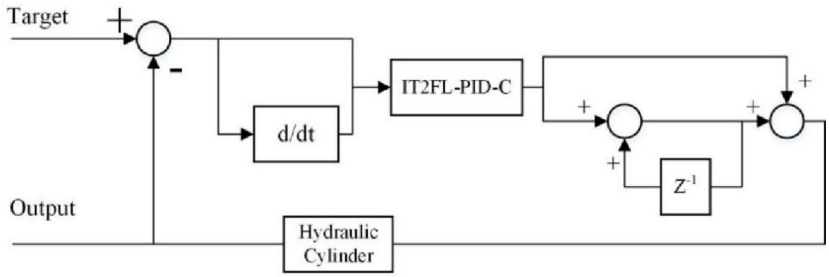

Fig. 4. IT2FL-PID-C system for hydraulic Cylinder.

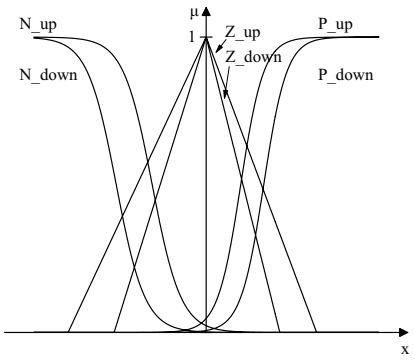

Fig. 5. MFs of IT2FL-PID-C for hydraulic system.

Inputs MFs for IT2FL-PID-C

Since cylinder performs differently in different strokes, four additional scaled parameters, $\overline{\mu_N}$, $\underline{\mu_N}$, $\overline{\mu_Z}$, $\underline{\mu_Z}$ are used to describe the input based on the symmetrical MFs. Equations (17)-(24) show the detailed formula, and Fig. 5 describes MFs of IT2FL-PID-C for the hydraulic system in our optimization, respectively.

$$Y_P = -Y_N k_s^{out} \tag{17}$$

$$Y_{PM} = -Y_{NM} k_s^{out} \tag{18}$$

$$\overline{\mu_N} = \frac{1}{1 + e^{(kk_s x - \frac{\lambda_1 + \lambda_2}{k_s})}} \tag{19}$$

$$\underline{\mu_N} = \frac{1}{1 + e^{(kk_s x + \frac{\lambda_1 + \lambda_2}{k_s})}} \tag{20}$$

$$\overline{\mu_Z} = \begin{cases} \max(1 - \frac{kx}{2\lambda_2(1-\lambda_3)}, 0) & x > 0 \\ \max(1 + \frac{kk_s x}{2\lambda_2(1-\lambda_3)}, 0) & x < 0 \end{cases} \tag{21}$$

$$\underline{\mu_Z} = \begin{cases} \max(1 - \frac{kx}{2\lambda_2(1+\lambda_3)}, 0) & x > 0 \\ \max(1 + \frac{kk_s x}{2\lambda_2(1+\lambda_3)}, 0) & x < 0 \end{cases} \tag{22}$$

$$\overline{\mu_P} = \frac{1}{1 + e^{-(kx - \lambda_1 + \lambda_2)}} \tag{23}$$

$$\underline{\mu_P} = \frac{1}{1 + e^{-(kx + \lambda_1 + \lambda_2)}} \tag{24}$$

Fuzzy rules for IT2FL-PID-C

The IT2FL-PID-C controller employed by this research institute utilizes a fuzzy rule base constructed based on the fundamental rules defined in Table 4. The general mathematical expression for this controller is provided by Eq. (25).

$$\mathrm{R}_n : IF\ E\ is\ \tilde{A}_j^1\ and\ \mathrm{d}E\ is\ \tilde{A}_j^2\ THEN\ y\ is\ Y_n \tag{25}$$

E/dE	*N*	Z	*P*
N	N	NM	Z
Z	NM	Z	PM
P	Z	PM	P

Table 4. Fuzzy rules of IT2FL-PID-C.

Where $n = 1, \ldots, 9$ denotes the number of rules, μ_n is the weighing factor to describe the significance of corresponding rule. The mapping from the type-1 MFs to type-2 MFs is achieved by introducing parametric uncertainty into the type-1 MF parameters. Specifically, Gaussian primary MFs with an uncertain standard deviation are employed. For a type-1 Gaussian MF is characterized by a fixed mean m and standard deviation σ, the corresponding type-2 MF is constructed by defining an uncertain standard deviation in the interval $[\sigma\ 1,\ \sigma\ 2]$, where $\sigma\ 1$ and $\sigma\ 2$ determine the lower MF (LMF) and upper MF (UMF), respectively. The region between the UMF and LMF constitutes the FOU. The size of the FOU is systematically determined. Heuristically, larger FOUs are allocated to linguistic values operating in regions where uncertainties are most pronounced, such as around "Zero" error, where stiction effects are critical. Subsequently, the exact parameters defining the FOUs are fine-tuned alongside the controller's scaling factors using the proposed ICBNDE optimization algorithm to minimize the performance index. This data-driven approach ensures that the FOUs quantitatively represent the effective uncertainties the controller must robustly address.

The 20 output MFs should be set for IT2FL-PID-C defuzzification for IT2FL-PID-C. Because more decision variables mean more difficulties in optimization, simplification is necessary in this IT2FL-PID-C. In literature[35,36], the researcher claimed that output MFs can be set to a constant value and used the same output MFs in up-MF and down-MF. Inspired by his method, simplification is used as Eqs. (26)-(28):

$$\underline{Y_N} = Y_N = \overline{Y_P} = \underline{Y_P} \tag{26}$$

$$\underline{Y_{NM}} = Y_{NM} = \overline{Y_{PM}} = \underline{Y_{PM}} \tag{27}$$

$$\underline{Y_Z} = Y_Z = 0 \tag{28}$$

The upper and lower dependency functions for all variables are set to equal values, eliminating iterative calculation and significantly improving the controller's response speed. Although simplifying the output MFs reduces computational load, it may limit the controller's expressive potential, which is a justified trade-off for this application. This simplification reduces the number of tunable parameters from 20 to 2 (effectively Y_P and Y_{PM} for PI and PD parts), drastically lowering the optimization search space dimensionality and computational cost. The potential performance ceiling imposed by this simplification is that the controller's ability to finely shape the nonlinear control law in the output domain is reduced. However, as demonstrated in Sect. 5.3 and the overall results, the optimized IT2FL-PID-C with simplified output MFs still achieves superior performance compared to PID and other MF types, indicating that for the targeted hydraulic system, the primary nonlinear compensation is effectively handled by the input MFs and rule base. The simplification is thus a pragmatic and effective engineering choice.

Defuzzification of IT2FL-PID-C

The defuzzification process holds the task of converting the generated type-2 fuzzy set to the actual output. In order to simplify the calculation, type reduction is necessary in IT2FL-PID-C. In this work, the type reduction method is applied, and the process of defuzzification can be summarized as Eqs. (29)-(38)[37]:

$$y_l^{(0)} = \frac{\sum_{i=1}^{M} \underline{f^i}(X)\, y_l^i}{\sum_{i=1}^{M} \underline{f^i}(X)} \tag{29}$$

$$y_l^{(M)} = \frac{\sum_{i=1}^{M} \overline{f^i}(X)\, y_l^i}{\sum_{i=1}^{M} \overline{f^M}(X)} \tag{30}$$

$$y_r^{(0)} = \frac{\sum_{i=1}^{M} \underline{f^i}(X)\, y_r^i}{\sum_{i=1}^{M} \underline{f^i}(X)} \tag{31}$$

$$y_r^{(M)} = \frac{\sum_{i=1}^{M} \overline{f^i}(X)\, y_r^i}{\sum_{i=1}^{M} \overline{f^i}(X)} \tag{32}$$

$$\overline{y}_l = \min(y_l^{(0)}, y_l^{(M)}) \tag{33}$$

$$\underset{-r}{y} = \max(y_r^{(0)}, y_r^{(M)}) \tag{34}$$

$$\underset{-l}{y} = \overline{y}_l - \left[\frac{\sum_{i=1}^{M} (\overline{f}^i - \underline{f}^i)}{\sum_{i=1}^{M} \overline{f}^i \sum_{i=1}^{M} \underline{f}^i} \times \frac{\sum_{i=1}^{M} \underline{f}^i (y_l^i - y_l^1) \sum_{i=1}^{M} \overline{f}^i (y_l^M - y_l^i)}{\sum_{i=1}^{M} \underline{f}^i (y_l^i - y_l^1) + \sum_{i=1}^{M} \overline{f}^i (y_l^M - y_l^i)} \right] \tag{35}$$

$$\overline{y}_r = \underset{-r}{y} - \left[\frac{\sum_{i=1}^{M} (\overline{f}^i - \underline{f}^i)}{\sum_{i=1}^{M} \overline{f}^i \sum_{i=1}^{M} \underline{f}^i} \times \frac{\sum_{i=1}^{M} \underline{f}^i (y_r^i - y_r^1) \sum_{i=1}^{M} \overline{f}^i (y_r^M - y_r^i)}{\sum_{i=1}^{M} \underline{f}^i (y_r^i - y_r^1) + \sum_{i=1}^{M} \overline{f}^i (y_r^M - y_r^i)} \right] \tag{37}$$

$$y = \frac{\underset{-l}{y} + \overline{y}_l + \underset{-r}{y} + \overline{y}_r}{4} \tag{38}$$

Where y denotes the output of IT2FLC, y_l^i and y_r^irepresent the outputs of the i-th rule.

Optimization of IT2FL-PID-C

After outlining the fundamental structure of the IT2FL-PID-C controller, its decision variables can be formally expressed as Eq. (39).

$$\mathrm{x} = \left\{ (k, \lambda_1, \lambda_2, \lambda_3, k_s)_E, (k, \lambda_1, \lambda_2, \lambda_3, k_s)_{dE}, (Y_P, Y_{PM})_{PI}, (Y_P, Y_{PM,})_{PD}, \right\} \tag{39}$$

As shown in this equation, the optimization problem involves 12 decision variables. Designing appropriate fitness and constraint functions for such optimization is crucial: the fitness function must not only directly reflect the system performance of IT2FL-PID-C but also possess favorable mathematical properties to reduce optimization complexity; the constraint function serves to confine controller parameters within a feasible domain. Given that step response performance and frequency response performance are the two most critical metrics in PID parameter tuning, this study designed a composite optimization objective centered on a frequency-performance-based fitness function and constrained by step-response performance. The specific expressions are shown in Eqs. (40) -(43).

$$\min : \mathrm{J} = \sum\nolimits_{i=0} ((Y_a^{cy}(i) - Y_d^{cy}(i))/\max(Y_d^{cy}))^2 \tag{40}$$

$$\text{sub to } \mathrm{h}_1 = \text{settling time} \leq \mathrm{t}_1 \tag{41}$$

$$\mathrm{h}_2 = \text{steady error} \leq \zeta_1 \tag{42}$$

$$Y_d^{cy}(i) = \begin{cases} 40 \times \sin(2\pi\, i/n) & i \leq 100 \\ 40 \times \sin(4\pi\, i/n) & 100 \leq i \leq 200 \\ 40 \times \sin(6\pi\, i/n) & 200 \leq i \leq 300 \end{cases} \tag{43}$$

Equation (40) is the fitness function of this IT2FL-PID-C, where $Y_a^{cy}(i)$ is the actual displacement and $Y_d^{cy}(i)$ is the desired displacement in the *i-th* sampling time. The desired displacement is designed with an increasing frequency to guarantee the optimized IT2FL-PID-C suit for more situations, and the description of Y_d^{cy} is shown in Eq. (43), where *n* denotes to sampling rates. Equations (41) and (42) are the constraint couple in this optimization. Settling time and steady error are important in cylinder control. The previous index can express the settling ability of IT2FL-PID-C, and the last denotes the accuracy of position. Six couples of these constraints are used in this optimization as shown in Table 5. To guarantee this IT2FL-PID-C's performance, six different response step experiments are tested. The targets of the indexes are similar in different strokes. The cylinder performs similarly to a symmetrical cylinder, which may benefit our further research.

Experiments and Analysis

In this section, the experiments about ICBNDE-based IT2FLC can be divided into three parts. Firstly, ICBNDE will be tested with benchmarks function to demonstrate its convergence ability. Then, ICBNDE based IT2FLC will be compared with the PID controller. This experiment will express the superiority of IT2FLC. Besides,

	1	2	3	4	5	6
Step displacement/mm	-100	-50	-25	25	50	100
Settling time/s	0.25	0.25	0.2	0.2	0.25	0.25
Steady error/mm	± 2	± 1	± 0.5	± 0.5	± 1	± 2

Table 5. Constraints of IT2FL-PID-C.

Instance	n	LI	NI	LE	NE	ρ	f
G01	13	9	0	0	0	0.011%	-15
G02	20	0	2	0	0	99.997%	-0.804
G03	10	0	0	0	1	0	-1.001
G04	5	0	6	0	0	51.123%	-30665.539
G05	4	2	0	0	3	0	5126.497
G06	2	0	2	0	0	0.007%	-6961.814
G07	10	3	5	0	0	0.001%	24.306
G08	2	0	2	0	0	0.856%	-0.096
G09	7	0	4	0	0	0.512%	680.630
G10	8	3	3	0	0	0.001%	7049.248
G11	2	0	0	0	1	0	0.749
G12	3	0	1	0	0	4.771%	-1
G13	5	0	0	0	3	0	0.054
G14	10	0	0	3	0	0	-47.765
G15	3	0	0	1	1	0	961.715
G16	5	4	34	0	0	0.020%	-1.905

Table 6. Details of benchmark test functions.

	G01	G02	G03	G04	G05	G06	G07	G08
Best	0.00E+00(0)	-2.46E-11(0)	9.00E-11(0)	-2.55E-11(0)	-1.82E-12(0)	3.37E-11(0)	-2.02E-11(0)	-1.80E-11(0)
Median	0.00E+00(0)	3.17E-10(0)	9.00E-11(0)	-2.55E-11(0)	-1.82E-12(0)	3.37E-11(0)	-2.02E-11(0)	-1.80E-11(0)
Worst	0.00E+00(0)	2.48E-09(0)	6.65E-10(0)	-2.55E-11(0)	-9.09E-13(0)	3.37E-11(0)	-2.02E-11(0)	-1.80E-11(0)
Mean	0.00E+00	4.40E-10	1.19E-10	-2.55E-11	-1.46E-12	3.37E-11	-2.02E-11	-1.80E-11
Std	0.00E+00	5.68E-10	1.14E-10	0.00E+00	4.55E-13	0.00E+00	1.33E-14	0.00E+00
Feasible Rate	100%	100%	100%	100%	100%	100%	100%	100%
Success Rate	100%	100%	100%	100%	100%	100%	100%	100%
	G09	**G10**	**G11**	**G12**	**G13**	**G14**	**G15**	**G16**
Best	1.71E-12(0)	-3.37E-11(0)	0.00E+00(0)	0.00E+00(0)	4.19E-11(0)	8.51E-12(0)	-3.91E-11(0)	-3.48E-11(0)
Median	1.82E-12(0)	-1.73E-11(0)	0.00E+00(0)	0.00E+00(0)	4.74E-11(0)	8.51E-12(0)	-3.91E-11(0)	-3.48E-11(0)
Worst	1.93E-12(0)	5.91E-11(0)	0.00E+00(0)	0.00E+00(0)	0.38E+0(0)	8.51E-12(0)	-3.91E-11(0)	-3.48E-11(0)
Mean	1.82E-12	-9.31E-12	0.00E+00	0.00E+00	0.03E+0	8.51E-12	-3.91E-11	-3.48E-11
Std	4.55E-14	2.56E-11	0.00E+00	0.00E+00	0.10E+0	1.97E-15	0.00E+00	0.00E+00
Feasible Rate	100%	100%	100%	100%	100%	100%	100%	100%
Success Rate	100%	100%	100%	100%	76%	100%	100%	100%

Table 7. Results of Benchmark Function Errors.

ICBNDE will also be compared with other meta-heuristic algorithms in IT2FLC designing. Through these experiments and analysis, the convergence ability of ICBNDE and its superiority in IT2FLC designing will be further proved.

Benchmark test of ICBNDE

The 16 benchmark test functions shown in Table 6 are employed to demonstrate the convergence ability of ICBNDE. All these benchmark tests are collected in the IEEE CEC2006 special session. ρ is the ration between the estimated feasible region and the search region. LI, NI, LE, NE denote the numbers of linearity inequality constraints, nonlinearity inequality constraints, linearity equality constraints and nonlinearity equality constraints respectively. f is the objective function value. When the error between f and value calculated by ICBNDE is less than E-4, this calculation will be treated as a successful searching process. The stop criterion used the maximum number of function evaluations (FES), and the FES for each function is set to 5*E5. All benchmark test functions will be tested 25 times. Some parameters used in this test are shown as follows: $Gro = 8$; $GroNP = 15$; $p = 0.3$ (functions with equality constraints) or $p = 0.2$ (functions without equality constraints).

Table 7 shows the results of benchmark function errors achieved by ICBNDE. The best error, median error, worst error of each benchmark function are shown, and the numbers of violated constraints are listed. What's more, the mean error, the std of errors, and the success rate are also listed in this table, from which we can summarize the convergence ability of ICBNDE. From Table 7, ICBNDE can find the best solution with a 100% feasible rate, which means that the selection strategy and greedy selection strategy work efficiently. During the

	IT2FL-PID-C	PID
Best	**0.551(0)**	1.643(0)
Median	**0.585(0)**	1.643(0)
Worst	**0.652(0)**	1.646(0)
Mean	**0.589**	1.643
Std	0.024	**8.833e-04**
Feasible Rate	**100%**	**100%**

Table 8. Results of ICBNDE in hydraulic controller design.

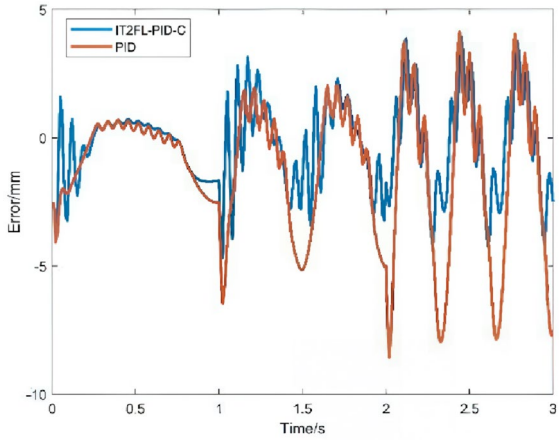

Fig. 6. Errors of IT2FL-PID-C and PID after optimization.

searching process, ICBNDE discards the solutions with worse constraint values and finally finds the feasible region finally. Like non-constraint meta-heuristic algorithm, selection strategy and greedy selection strategy may also lead to premature convergence in the searching process, which means that the algorithm may get trapped in a local optimal solution easily. Simultaneously, the success rate is also an important index to measure the searching ability of ICBNDE. ICBNDE can exactly find the best results with a 100% success rate for most benchmark functions. For G13, ICBNDE can find the best result with a 76% success rate. To our known, G13 has a local optimal solution with the value 0.4388, and nearly all the cases (23/25) jump out of this solution. G02 is the benchmark function with the most local optimal solutions. ICBNDE can find the best solution in all the cases. During the searching process, the individuals of ICBNDE are divided into several groups, and the operation is implemented group by group. This mechanism can be treated as a niching strategy, and it enhances the global search ability of ICBNDE directly. Through this experiment, we can conclude that ICBNDE is featured with strong convergence ability and is expected to perform well in IT2FL-PID-C design.

Performance of ICBNDE based IT2FL-PID-C in hydraulic system

This section first employs the ICBNDE algorithm to optimize the IT2FL-PID-C controller. For comparative purposes, the same objective and constraint functions are applied to optimize a conventional PID controller for the hydraulic system using ICBNDE. Subsequently, the performance of the IT2FL-PID-C controller is evaluated and compared against the PID controller. To ensure a fair comparison and reliable statistical analysis, the maximum number of function evaluations (FES) for both simulations is set to 1.5×10^5, with all configuration parameters remaining identical to those in the previous experiment. ICBNDE is independently executed 20 times for both the IT2FL-PID-C and PID controller designs.

Table 8 presents the best, median, mean, standard deviation, and feasibility rate of all optimization results, with the number of constraint violations indicated in parentheses. The results show that ICBNDE obtains solutions fully satisfying the constraints for both controller types, demonstrating its suitability for designing both IT2FL-PID-C and PID controllers in hydraulic systems. Furthermore, the fitness function value achieved for the IT2FL-PID-C is smaller. Since the fitness function is defined as the sum of squared relative errors, a smaller value indicates lower tracking error in the frequency test. Figure 6 illustrates the displacement error between the actual and target trajectories for the median solution during the frequency test. For most of the time, the IT2FL-PID-C exhibits smaller errors than the PID controller. This is attributed to the asymmetric nature of the hydraulic cylinder, which linear PID control cannot optimally accommodate in both extending and retracting strokes. Therefore, it can be concluded that the IT2FL-PID-C outperforms the PID controller in the hydraulic cylinder system. The IT2FL-PID-C exhibits a more intermittent or higher-frequency control action compared to the smoother PID response. This characteristic can be interpreted as the fuzzy logic controller actively compensating for the asymmetric nonlinearity of the hydraulic cylinder. The IT2FL-PID-C, with its

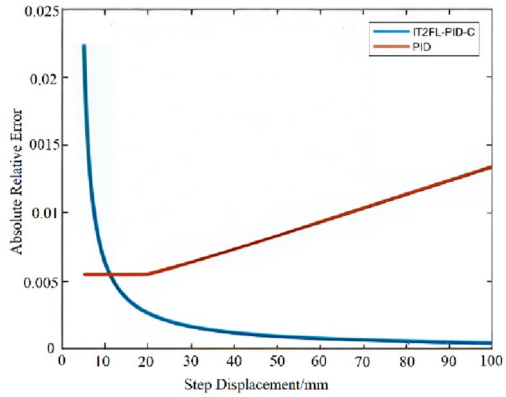

Fig. 7. Absolute relative error of positive step.

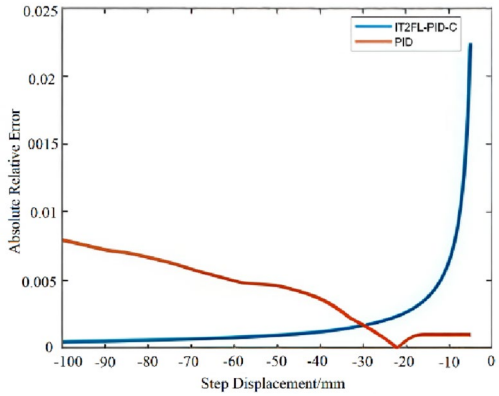

Fig. 8. Absolute relative error of negative step.

nonlinear mapping capability, adjusts its output more aggressively and frequently to counteract these varying dynamics, leading to smaller overall tracking error but a busier control signal. Though Fig. 6a shows highly intermittent response. This is primarily due to the aggressive tuning of the controller's parameters to prioritize rapid rise time and minimal overshoot. While this results in a higher frequency of control action, it successfully eliminates the significant overshoot and oscillation seen in the PID response.

To further analyze the step response performance of the IT2FL-PID-C, an additional experiment is conducted. The hydraulic cylinder system under IT2FL-PID-C control is simulated with target displacements ranging from 5 to 95 mm (positive) and −5 to -95 mm (negative), while the settling time and absolute relative steady-state error are recorded. These two metrics, also used in the constraint design, are critical for the hydraulic cylinder in our humanoid robot. For comparison, the hydraulic system under PID control is also simulated under the same conditions using the median optimized solutions.

Figures 7, 8, 9 and 10 show the results of the step test. From Fig. 7, when the target displacement is small, the absolute relative steady error of IT2FL-PID-C is large. When target displacement increases, the absolute relative steady error of IT2FL-PID-C decreases. While the performance of PID is different, the absolute and relative steady error of PID increases with the target displacement increasing. The absolute relative steady error of IT2FL-PID-C is smaller than PID when the target displacement is bigger than 12 mm or smaller than −30 mm. Figure 8 also shows a similar phenomenon when the target displacement is negative. Figures 9 and 10 show the settling time of the step test. It's noticed that when the displacement is bigger than −7 mm or smaller than 7 mm, the settling time is equal to 0.2s. Because the criterion of settling time is that the actual displacement sits between 0.98*target displacement and 1.02*target displacement. The relative steady error of IT2FL-PID-C in these areas is above 2% as we can see in Figs. 7 and 8, so the total simulation time is recorded as their settling time. What's more, the settling time of PID is a bit less than that of IT2FL-PID-C in most cases.

In summary, the ICBNDE-based optimization method is effective for both IT2FL-PID-C and PID controller tuning in hydraulic systems. After optimization with ICBNDE, the IT2FL-PID-C demonstrates superior performance in frequency response and steady-state error, while the PID controller performs slightly better in settling time.

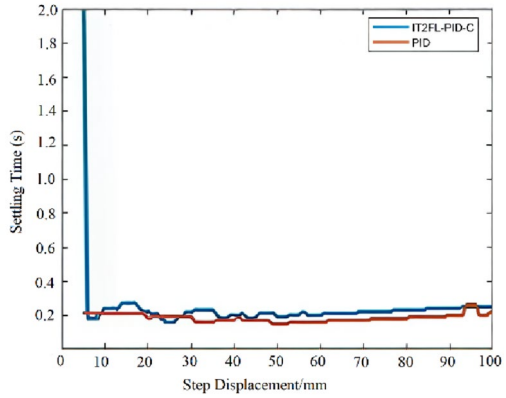

Fig. 9. Settling time of positive step.

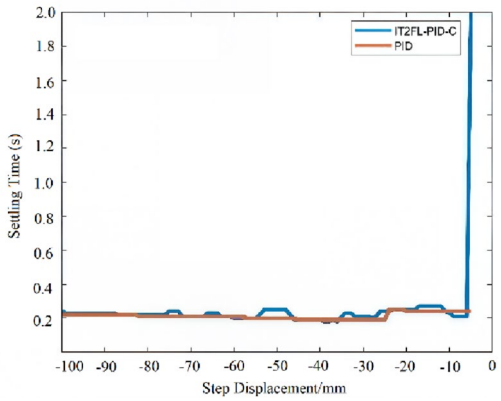

Fig. 10. Settling time of negative step.

Performance Index	Triangular	Gaussian	Trapezoidal
ITSE	1.153	**0. 637**	1.984
IAE	1.762	**1.336**	2.682
Overshoot	12.48%	**4.29%**	16.93%
Setting time(s)	0.67	**0.44**	0.76
Steady-state error	0.047	**0.017**	0.032

Table 9. Performance comparison under different input MFs.

Comparative analysis of different MFs

The comparative analysis is conducted to evaluate the impact of different MF shapes on the performance of the proposed IT2FL-PID-C controller. Three common MF types—Triangular, Gaussian, and Trapezoidal—are designed for the input variables[38]. The output MFs remain simplified as Eqs. (26)-(28) to maintain computational efficiency. All three controllers are optimized using our proposed ICBNDE under the same conditions and performance index.

The comparative results are summarized in Table 9. It is observed that the Gaussian MFs yield the best overall performance, achieving not only the smallest integral of time-weighted square error (ITSE) but also demonstrating superior characteristics in key transient and steady-state metrics. The Gaussian MFs yield the lowest integrated absolute error (IAE), indicating superior overall tracking accuracy. Furthermore, they achieve the most stable transient response, as evidenced by a significantly reduced overshoot of merely 4.29%, which is approximately one-third of that observed with the Triangular MFs and one-fourth of the Trapezoidal MFs' overshoot. This excellent stability is complemented by the fastest dynamic response, with a settling time of 0.44 s, outperforming both the Triangular and Trapezoidal configurations. Finally, the Gaussian MFs also provide the best steady-state precision, achieving a near-zero steady-state error.

Algorithms	Parameters
RCGA	$N = 100;\ P_c = 0.9;\ P_m = 0.1;\ \lambda$=0.1; $Cl = 10^6;\ CE = 10^7;$
DMS-PSO	ω=0.729, $C1 = C2 = 1.49445;\ n = 20;\ ns = 3;\ R = 100;\ L = 500;$
CDE	$NP = 50;\ F = 0.7;\ Cr = 0.9;$
ConSADE	$F = \{0,2\};\ Gro = 8;\ GroNP = 15;\ p = 0.3$
CMODE	$\lambda = 8;\ k = 22;\ NP = 70;\ F = \{0.5,0.6\};\ Cr = \{0.9,0.95\};$
DPDE	$SN = 100;\ F = 0.8;\ Cr = 0.9;$

Table 10. Parameters of compared algorithms.

	IT2FL-PID-C	RCGA	DMS-PSO	CDE	ConSADE	CMODE	DPDE
Best	0.5511(0)	0.5675(0)	0.5774(0)	0.5348(0)	0.6378(0)	0.5392(0)	0.5648(0)
Median	**0.5852(0)**	1.0234(0)	0.6597(0)	2.3027(0)	2.4047(0)	0.6220(0)	0.6350(0)
Worst	**0.6526(0)**	3.9639(0)	0.7255(0)	2.5232(0)	3.0688(0)	0.6607(0)	3.0200(0)
Mean	**0.5888**	1.7079	0.6498	1.5705	1.8875	0.6115	1.2297
Std	**0.0239**	1.1711	0.0359	0.9397	0.8906	0.0339	0.8997
Feasible Rate	**100%**	**100%**	**100%**	**100%**	**100%**	**100%**	**100%**

Table 11. Results of ICBNDE and compared algorithms.

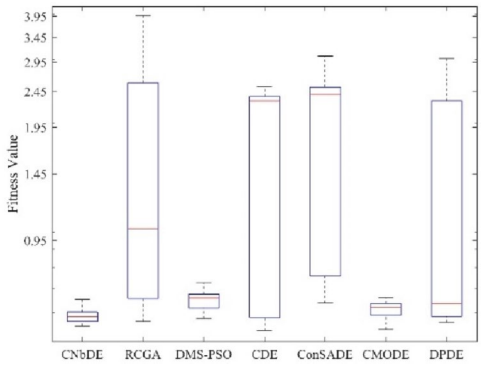

Fig. 11. Box plot of ICBNDE and other compared algorithms.

In summary, the Gaussian MFs consistently outperform both the Triangular and Trapezoidal variants by delivering a more accurate, stable, and rapid response. Therefore, the Gaussian membership function is confirmed as the optimal choice for the IT2FL-PID-C controller in this hydraulic servo system application.

Comparison between ICBNDE and other algorithms

After previous experiments and analysis about ICBNDE-based IT2FL-PID-C optimization, the feasibility of ICBNDE in IT2FL-PID-C has been proved. Many constraint meta-heuristic algorithms also perform well in benchmark functions tests, so the research of other constraint meta-heuristic algorithms in IT2FL-PID-C are of great value. This section mainly concerns the comparison between ICBNDE and several other algorithms in IT2FL-PID-C optimization. Six different constraint algorithms, including RCGA[39], DMS-PSO[40], CDE[41], ConSADE[42], CMODE[43], and DPDE[44], are also implanted in IT2FL-PID-C optimization. RCGA is GA based constraint optimization method, and DMS is PSO based constraint optimization method. GA and PSO are the most popularly used in non-constraint IT2FL-PID-C problems, so in this paper, RCGA and DMS-PSO are listed in the compared algorithms. CDE and ConSADE are the classical constraint DE, CMODE and DPDE are the constraint DE proposed recently, so comparison between ICBNDE and them are meaningful. For fairly comparison, all algorithms are implemented with the 1.5*E5 FES and 20 times. The basic parameter settings for each algorithm remain unchanged from the original text are as shown Table 10. The default configurations of these algorithms are shown as follows:

Table 11 shows the results achieved by ICBNDE and other compared algorithms, and Fig. 11 shows the box plot of these results. From Table 11, we can see that all the algorithms can achieve a feasible solution with 1.5*E5 FES, and ICBNDE achieves the best result in median solution, worst solution, mean solution, std of solutions. It can be seen from Fig. 11, the dispersion degree of mean fitness values of optima found by ICBNDE is relatively smaller compared with other algorithms. A nuanced analysis reveals an important trade-off: while

algorithms like CDE and CMODE occasionally found a slightly better "best" solution (lower minimum fitness), ICBNDE demonstrated superior consistency and reliability. It achieved the best median, mean, and worst-case performance, along with the smallest standard deviation. This indicates that ICBNDE is less sensitive to initial conditions and random seeds, providing more repeatable and robust optimization outcomes. For engineering applications where reliable and predictable controller performance across multiple design runs is paramount, ICBNDE's robustness is a significant advantage over its ability to sporadically find a marginally better optimum. Based on these analyses, we can conclude that ICBNDE performs better in IT2FL-PID-C compared with other algorithms.

Conclusion

For the optimization problem of a zone-type fuzzy PID controller in the hydraulic cylinder system of humanoid robots, this paper proposes a meta-heuristic optimization method based on a constraint processing mechanism. Unlike most meta-heuristic algorithms that rely on parameter tuning, this method exhibits parameter-independent characteristics. A novel constrained meta-heuristic algorithm—ICBNDE—is further designed and applied to the optimization design of this controller. Simulation results demonstrate ICBNDE's superior performance on standard constrained benchmark problems, validating its effectiveness for constrained optimization. Concurrently, the feasibility of the IT2FL-PID-C optimization scheme is confirmed. Regarding hydraulic cylinder control performance, compared to the classical PID controller, the IT2FL-PID-C demonstrates advantages in both frequency response characteristics and steady-state error control, while the PID controller slightly outperforms in stability time metrics. More importantly, in this specific optimization problem, ICBNDE outperforms multiple classical constrained meta-heuristic algorithms, indicating its stronger adaptability and solution capability for such problems.

Although ICBNDE based IT2FL-PID-C is featured with easy implement. Limitation of this method also exists. Firstly, the performance of ICBNDE should be further improved, because the simulation results show that CMODE and CDE performs better in the index of best solution. So the improvement of ICBNDE could be a topic of further research. What's more, meta-heuristic algorithm based IT2FL-PID-C methods also lead to huge time costs, especially when the sampling rate is higher. In our future research, surrogate-assisted method will be introduced in IT2FL-PID-C optimization. Specifically, efficient surrogate models such as Kriging (Gaussian Process) or Radial Basis Function networks could be integrated to approximate the expensive fitness function evaluations, thereby significantly reducing computational burden. Future extensions could also explore integrating the optimized IT2FL-PID-C with advanced robust control frameworks, such as those addressing servo constraint following for complex manipulation tasks[45], to enhance performance in dynamic and uncertain environments.

Data availability

The datasets used and/or analysed during the current study available from the corresponding author on reasonable request.

Received: 3 November 2025; Accepted: 18 February 2026
Published online: 25 February 2026

References

1. Aaboud, M. Electron efficiency measurements with the ATLAS detector using 2012 LHC proton–proton collision data [J]. *Eur. Phys. J. C*. **77** (3), 195 (2017).
2. Ding, L., Wang, R. & Feng, H. Key Technology Analysis of Big Dog Quadruped Robot [J]. *Mech. Eng.* **51**, 1–23 (2015).
3. Ugurlu, B. et al. Pattern generation and compliant feedback control for quadrupedal dynamic trot-walking locomotion: experiments on RoboCat-1 and HyQ [J]. *Auton. Robots*. **38** (4), 415–437 (2015).
4. Budde, L., Hundertmark, J. & Meyer, T. HYBERFLOW-enabling non-invasive flow rate feedback control in bioprinting via hydraulic actuation [J]. *Bioprinting* **50**, e00435 (2025).
5. Aliskan, I. The optimization-based fuzzy logic controllers for autonomous ground vehicle path tracking [J]. *Eng. Appl. Artif. Intell.* **151**, 110642 (2025).
6. Wang, Q., Cao, J. D. & Liu, H. Adaptive fuzzy control of nonlinear systems with predefined time and accuracy[J]. *IEEE Trans. Fuzzy Syst.* **30** (12), 5152–5165 (2022).
7. Zhang, T. et al. An innovative coordinated control strategy for frequency regulation in power systems with high renewable penetration [J]. *Appl. Energy*. **401**, 126770 (2025).
8. Kumar, A. & Kumar, V. Evolving an interval type-2 fuzzy PID controller for the redundant robotic manipulator [J]. *Expert Syst. Appl.* **73**, 161–177 (2017).
9. Mansoor, Z. & Gharibi, A. Applications of type-2 fuzzy logic system: handling the uncertainty associated with candidate-well selection for hydraulic fracturing [J]. *Neural Comput. Appl.* **27** (7), 1831–1851 (2016).
10. Sajadinia, M. An adaptive virtual inertia control design for energy storage devices using interval type-2 fuzzy logic and fractional order PI controller [J]. *J. Energy Storage*. **84**, 110791 (2024).
11. Kumar, A. et al. *Design of a novel mixed interval type-2 fuzzy logic controller for 2-DOF robot manipulator with payload [J]* Vol. 123, 106329 (Engineering Applications of Artificial Intelligence, 2023).
12. Naik, K., Gupta, C. & Fernandez, E. Design and implementation of interval type-2 fuzzy logic-PI based adaptive controller for DFIG based wind energy system [J]. *Int. J. Electr. Power Energy Syst.* **115**, 105468 (2020).
13. Maldonado, Y., Castillo, O. & Melin, P. A multi-objective optimization of type-2 fuzzy control speed in FPGAs [J]. *Appl. Soft Comput.* **24**, 1164–1174 (2014).
14. Li, C., Zhang, X. & Yi, J. SIRMs connected type-2 fuzzy-genetic backing up control of the truck-trailer system [J]. *Proceedings of the 31st Chinese Control Conference.* (IEEE, 2012).
15. Hamza, F., Yap, H. & Choudhury, I. Genetic algorithm and particle swarm optimization based cascade interval type 2 fuzzy PD controller for rotary inverted pendulum system [J]. *Mathematical Problems in Engineering*, **2015**, 695965 (2015).
16. Allawi, Z. & Turki, Y. A PSO-optimized type-2 fuzzy logic controller for navigation of multiple mobile robots [J]. *2014 19th international conference on methods and models in automation and robotics (MMAR)*. (IEEE, 2014).

17. Kiani, M., Seyed, M. & Gharaveisi, A. A bacterial foraging optimization approach for tuning type-2 fuzzy logic controller [J]. *Turkish J. Electr. Eng. Comput. Sci.* **21** (1), 263–273 (2013).
18. Fayek, H. et al. A controller based on Optimal Type-2 Fuzzy Logic: Systematic design, optimization and real-time implementation [J]. *ISA Trans.* **53** (5), 1583–1591 (2014).
19. Arega, T. B., Tesfa, Y. M. & Abdissa, C. M. Three-wheeled mobile robot trajectory tracking control using nonlinear PID controller based neural network combined with backstepping controller [J]. *IEEE ACCESS.* **13**, 100167–100182 (2025).
20. Nasiri, K., Moradi, H. & Arora Chatter suppression in nonlinear milling of a flexible plate-workpiece with attached piezoelectric actuators: Comparison of soft-actor-critic-based controller vs optimized type-2 fuzzy controller [J]. *Mech. Syst. Signal Process.* **224**, 112198 (2025).
21. Abdessamad, E., Kouiss, K. & Chebak, A. Total energy control system-based interval type-3 fuzzy logic controller for fixed-wing unmanned aerial vehicle longitudinal flight dynamics [J]. *Aerosp. Sci. Technol.* **162**, 110253 (2025).
22. Oubelaid, A. et al. Adaptive hierarchical smoothing strategy and fuzzy logic-based torque vectoring algorithm for comfort and propulsion optimization in over-actuated hybrid electric vehicles[J]. *Results Eng.* **27**, 106289 (2025).
23. Ren, H. & Gong, P. Adaptive control of hydraulic position servo system using output feedback [J]. *Proceedings of the Institution of Mechanical Engineers, Part I: Journal of Systems and Control Engineering*, **231**(7), 527–540 (2017).
24. Abdesattar, M. et al. Comprehensive optimization of fuzzy logic-based energy management system for fuel-cell hybrid electric vehicle using genetic algorithm [J]. *Int. J. Hydrog. Energy*. **81**, 889–905 (2024).
25. Gao, B. et al. Research on decoupling control of single leg joints of hydraulic quadruped robot [J]. *Robotic Intell. Autom.* **44** (2), 201–214 (2024).
26. Dong, H. et al. Differential Evolution with Better and Nearest Option for Function Optimization. *2019 IEEE Congress Evolutionary Comput. (CEC)*. (IEEE, 2019).
27. Fang, L. et al. Open-source lower controller for twelve degrees of freedom hydraulic quadruped robot with distributed control scheme [J]. *HardwareX* **13**, e00393 (2023).
28. Abualigah, L. et al. Improved synergistic swarm optimization algorithm to optimize task scheduling problems in cloud computing [J]. *Sustainable Computing: Inf. Syst.* **43**, 101012 (2024).
29. Hu, Z., Cai, X. & Fan, Z. An improved memetic algorithm using ring neighborhood topology for constrained optimization [J]. *Soft. Comput.* **18** (10), 2023–2041 (2014).
30. Li, X. & Yin, M. Self-adaptive constrained artificial bee colony for constrained numerical optimization[J]. *Neural Comput. Appl.* **24** (3–4), 723–734 (2014).
31. Mohammed, H., Mostafa, B., Mohammed, A. & PSO-Optimized IT2FLC for load frequency and VRFB control in two-area interconnected power system [J]. *Results Eng.* **27**, 106107 (2025).
32. Dong, L. et al. Feasibility-guided search and prediction for dynamic constrained multiobjective evolutionary optimization [J]. *Swarm Evol. Comput.* **99**, 102157 (2025).
33. Chen, W. et al. *A decomposition-based evolutionary algorithm with multiple reference points strategy for multiobjective optimization [J]* (European Journal of Operational Research, 2025). Available online.
34. Kamal, D. & Manoj, T. Multiobjective evolutionary algorithm based wrapper approach for hyperspectral band selection [J]. *Eng. Appl. Artif. Intell.* **159**, 111631 (2025).
35. Huo, Z. et al. Adaptive event-triggering mechanism based Takagi-Sugeno fuzzy automatic generation controller design for offshore wind power system[J]. *Ocean Eng.* **302**, 117602 (2024).
36. Mortazavi, A. A novel binomial-based fuzzy type-2 approach for topology and size optimization of skeletal structures[J]. *Adv. Eng. Softw.* **199**, 103819 (2025).
37. Long, N. & Le, T. Type-2 interval-valued fuzzy reservoir network for autolanding control under uncertainty [J]. *Results Eng.* **28**, 107319 (2025).
38. Nisha, K., Pulakraj, A. & Lloyds, G. Dual degree branched type-2 fuzzy controller optimized with a hybrid algorithm for frequency regulation in a triple-area power system integrated with renewable sources [J]. *Prot. Control Mod. Power Syst.* **8**, 48 (2023).
39. Chuang, Y., Chen, C. & Hwang, C. A simple and efficient real-coded genetic algorithm for constrained optimization [J]. *Appl. Soft Comput.* **38**, 87–105 (2016).
40. Bagheri, A., Jabbariet, A. & Mobayen, S. An intelligent ABC-based terminal sliding mode controller for load-frequency control of islanded micro-grids. *Sustainable Cities Society[J]*. **64**, 102544 (2021).
41. Xu, T., Chen, H., He & Jun An adaptive helper and equivalent objective evolution strategy for constrained optimization [J]. *Inf. Sci.* **690**, 121184 (2025).
42. Lu, Y. et al. A multi-strategy self-adaptive differential evolution algorithm for assembly hybrid flowshop lot-streaming scheduling with component sharing [J]. *Swarm Evol. Comput.* **92**, 101783 (2025).
43. Sallam, K. et al. Landscape-assisted multi-operator differential evolution for solving constrained optimization problems [J]. *Expert Syst. Appl.* **162**, 113033 (2020).
44. Gao, W., Gary, G. & Liu, S. A dual-population differential evolution with coevolution for constrained optimization [J]. *IEEE Trans. cybernetics*. **45** (5), 1108–1121 (2014).
45. Liu, X. et al. Robust Control under Servo Constraint Following via Nash Equilibrium Theory for Bimanual[]Humanoid Manipulation. [J]. *IEEE Trans. Fuzzy Syst.* **33** (11), 4069–4082 (2025).

Author contributions

Xin Chen: Project administration, Resources, Software, Writing – original draft. Hongzhen Dong: Data curation, Conceptualization, Methodology, Control method, Writing – review & editing. Chen Shen: Conceptualization, Supervision. Hanyu Li: Methodology, Modeling, Writing – review & editing. Dong Li: Writing – review & editing, Funding acquisition.

Funding

This research is supported by Hubei Province Natural Science Foundation of China under Grant No. 2023AFB395.

Declarations

Competing interests

The authors declare no competing interests.

Additional information

Correspondence and requests for materials should be addressed to D.L.

Reprints and permissions information is available at www.nature.com/reprints.